RSC Advances

ROYAL SOCIETY OF CHEMISTRY

www.rsc.org/advances

Oxygen-doped activated carbons derived from three kinds of biomasses: Preparation, characterization and performance as electrode materials for supercapacitors

Wanru Feng[1] Ping He*[1] Shuangshuang Ding[1] Guangli Zhang[1] Mingqian He[2] Faqin Dong[3] Jianwu Wen[1] Licheng Du[1] Mingzhang Liu[2]

1 State Key Laboratory Cultivation Base for Nonmetal Composites and Functional Materials, School of Materials Science and Engineering, Southwest University of Science and Technology, Mianyang 621010, Sichuan, P. R. China

2 Sichuan Changhong Battery Co., Ltd, Mianyang 621010, Sichuan, P. R. China

3 Key Laboratory of Solid Waste Treatment and Resource Recycle of Ministry of Education, Southwest University of Science and Technology, Mianyang 621010, Sichuan, P. R. China

Abstract: In this work, oxygen-rich activated carbon compounds were prepared from three kinds of biomasses by simple carbonization and they were investigated as electrodes for supercapacitors. The selected biomasses were waste dragon fruit skin, momordica grosvenori skin and firmiana catkins. Three kinds of as-prepared activated carbons showed abundant oxygen-containing groups and typical amorphous characteristics with high specific surface areas of 911.2 m^2 g^{-1}, 597.5 m^2 g^{-1} and 286.7 m^2 g^{-1}, respectively. This combination of high specific surface areas and abundant active surface functional groups resulted in capacitance of 286.9 F g^{-1}, 238.7 F g^{-1} and 226.6 F g^{-1} at 0.5 A g^{-1}, respectively. Furthermore, three kinds of as-prepared activated carbons also showed excellent cycling performance with nearly 100% retention over 5000 cycles at 4.0 A g^{-1} in 2.0 mol l^{-1} KOH solution. As a result, three kinds of as-prepared activated carbons exhibited favorable

* Corresponding author. Tel.: 86-816-6089371. E-mail: heping@swust.edu.cn.

electrochemical performances in potential application as electrode materials for supercapacitors.

Keywords: supercapacitors; specific capacitance; biowaste; activated carbons

1. Introduction

As the intermediate devices between conventional batteries and dielectric capacitors, supercapacitors have attracted more and more attention due to their safety, short charging time and electrochemical stability.[1,2] Nowadays, supercapacitors are widely used in consumer electronics, electric vehicles, pulsing techniques, industrial power and energy management.[3-5] The energy storage in supercapacitors is based on ion adsorption (electrical double-layer capacitors, EDLCs) or reversible faradaic reactions (pseudo-capacitors).[6] Pseudo-capacitive materials, mainly metal oxides and electrical conductive polymers, have been used as high specific capacitance electrodes and, however, they still have some poor characteristic, such as low conductivity, poor cycle stability and high cost. Various carbon materials, such as graphene,[7] carbon nanotubes,[8] activated carbons (ACs),[9] carbon aerogel[10] and carbon composites,[11] are widely employed as electrode materials for supercapacitors because of their good electrical conductivity, electrochemical stability and natural abundance.

Considering the potential scale of supercapacitor applications, the development of low-cost carbon materials from renewable raw materials is even more worthwhile. Biomass materials are renewable, easily available and very cheap, which are potential raw materials for the preparation of porous carbons with good capacitive performance.[12,13] Among a variety of tested materials, biochar samples derived from woody mass showed a specific surface area of 1000 $m^2\ g^{-1}$ and a specific capacitance of 167 F g^{-1}.[14] Activated carbon prepared from rice hulls showed a specific capacitance of 368 F g^{-1}.[15] Recently, distiller-dried grains derived hierarchical carbon had a high specific surface area of 3000 $m^2\ g^{-1}$ and a specific capacitance of 260 F g^{-1}.[16]

The choices of carbon precursors and activation conditions determine electrochemical

performances because specific surface area and presence of electrochemically active surface functional groups can affect double-layer capacitances.[17] Previous studies have proved that surface heteroatom-containing groups such as oxygen or nitrogen can give ACs acid/base characteristics. Therefore, those heteroatom-containing groups play a critical role in enhancing capacitance performances via revisable redox reaction together with improved wettability between electrode and electrolyte. Chemical activation is generally made by mixing carbonaceous materials with chemical activating agents (KOH, H_3PO_4, $ZnCl_2$, etc), followed by carbonization at 400 ~ 900 ℃. Among these agents, KOH has been widely used since it can result in ACs with defined micropore size distribution and high specific surface areas (SSAs). Besides, KOH activation is also efficient for generating mesopores into the framework of various structured carbons.

Waste dragon fruit skin (DF),[18] momordica grosvenori skin (MG)[19] and firmiana catkins (FC) are of particular interest with the virtue of low cost, abundance, availability and environmental friendliness, making them ideal candidates for preparing ACs. Until now no published literature showed synthesis of oxygen-rich ACs as electrode materials for supercapacitors from DF, MG or FC.

In this work, we for the first time demonstrate the fabrication of DF, MG and FC-derived oxygen-rich ACs by high-temperature carbonization and KOH activation under argon atmosphere. The electrochemical properties of as-prepared ACs were assessed by cyclic voltammetry (CV) and galvanostatic charge/discharge (GCD).

2. Experimental

2.1 Preparation of ACs

DF, MG and FC were collected from local place. These biomass materials above were washed thoroughly with water to remove soil and clay and then dried at 60 ℃ in an oven for 48 h. Afterwards, carbonization and KOH activation of DF, MG and FC were carried out as follows. Briefly, DF, MG and FC were carbonized at temperature of 500 ℃ for 1 h in an argon flow of 40 cm^3 min^{-1}, and then three kinds of carbonized carbons (denoted as X-C, X as DF, MG and FC) were obtained.

Subsequently, a given mass of X-C was impregnated in 3.0 mol l^{-1} KOH solution for 24 h (mass ratio of KOH/X-C was 3), followed by an evaporation step at 80 ℃ under vacuum atmosphere. The dried KOH-treated X-C was heated at 800 ℃ for 1 h in an argon flow of 40 cm^3 min^{-1} in a horizontal tube furnace. After being cooled down to room temperature in flowing argon flow, as-obtained product was neutralized by 1.0 mol l^{-1} HCl solution until pH reached 7.0. Subsequently, as-prepared ACs (denoted as DF-AC, MG-AC and FC-AC) were filtered, washed with deionized water and dried at 60 ℃ in ambient for 10 h.

2.2 Structural characterization of X-ACs

The morphology and structure of X-ACs were studied using field emission scanning electron microscopy (SEM) (JSM-6360LV, Japan).

A surface area and porosity analyser (Micromeritics ASAP 2020, USA) was employed in N_2 adsorption-desorption (77 K) analysis to obtain the N_2 adsorption isotherms of X-ACs. X-ACs were degassed at 300 ℃ under vacuum for 12 h prior to measurement. Brunauer-Emmett-Teller (BET) and Horvath-Kawazoe (HK) were used to calculate the specific surface area and the pore size distribution, respectively.

X-ray diffraction (XRD) measurements of X-AC were carried out using X-ray diffractometer (XRD, X' Pert Pro, Philips) using a graphite monochromator with Cu K_α radiation (λ = 1.5406 Å). The XRD data were collected between scattering angles (2θ) of 3° to 80° at a scanning rate of 4° min^{-1}.

Chemical characterization of functional groups of X-ACs was detected by Fourier transform infrared (FTIR) spectrometer (Nicolet 5700 Instrument Co., USA) using KBr method in the scanning range of 4000–400 cm^{-1}.

Raman spectra of X-ACs were recorded by Lab RAM HR800 (JY Horiba, France) with a 532 nm laser excitation.

The surface chemical species of as-prepared X-ACs were examined on Perkin-Elmer PHI-5702 multifunctional X-ray photoelectron spectroscope (XPS, Physical Electronics, USA) using Al K_α radiation of 1486.6 eV as excitation source. All XPS spectra were calibrated using Au $4f_{7/2}$ at 84.0 eV.

2.3 Electrodes preparation and electrochemical measurements

Electrodes for supercapacitors were prepared by mixing electroactive as-prepared X-AC materials with 10 wt.% acetylene black and 10 wt.% polytetrafluoroethylene emulsion to make homogeneous slurry. The obtained slurry was pressed onto a piece of nickel foam with an apparent area of 1 cm^2 under the pressure of 5.0 MPa. The pasted nickel foam was then dried at 80 ℃ in vacuum for 24 h.

All experiments were carried out at room temperature (23 ± 2 ℃) using KOH solution (2.0 mol l^{-1}) as an electrolyte. All electrochemical measurements were carried out by introducing a three-electrode test system using platinum sheet as counter electrode, as-prepared X-AC electrode as working electrode and Hg/HgO electrode as reference electrode. CV and GCD tests were recorded between −1.0 ~ 0 V using PARSTAT 2273 electrochemical workstation (Princeton Applied Research, USA).

3. Results and discussion

3.1 Structure and morphology of as-prepared X-ACs

SEM images (Fig. 1a, 1b and 1c) showed irregular, amorphous structure with a mountain of channels (the insets) in the surface of as-prepared X-ACs. The width of those channels was less than 10 nm, providing favorable paths for transportation of electrolyte ions, and thus increasing the contact areas between electrode materials and electrolyte. These channels in as-prepared X-ACs might be attributed to the evaporation of KOH which left space during activation as well as the subsequent removal of untreated KOH by washing with deionized water.

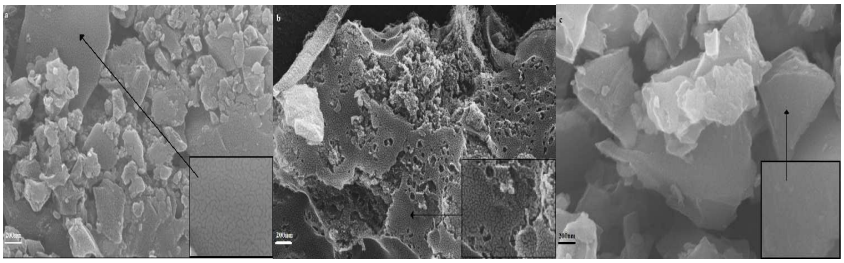

Fig. 1 SEM images of DF-AC (a), MG-AC (b) and FC-AC (c)

Shown in Fig. 2a were the N_2 adsorption/desorption isotherms of the different samples. All the samples exhibited typical characteristics of type-IV isotherms with hysteresis loop, showing a combination of microporous-mesoporous structure.[20] In

the range of 0.4 ~ 0.9 (relative pressure, P/P_0), DF-AC exhibited more obvious hysteresis than that of MG-AC or FC-AC, indicating the presence of abundant mesopores on the surface of DF-AC.

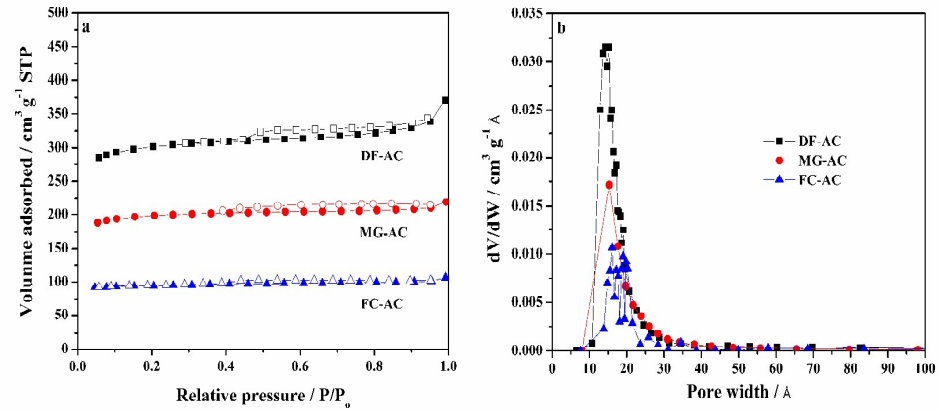

Fig. 2 N_2 adsorption-desorption isotherms (a) and HK pore size distribution (b) of as-prepared X-ACs

It was well known that the energy storage occurred primarily in micropores. However, only micropores structure would limit the increase in electric double-layer capacitance because it was difficult for inner pores to be fully accessed by electrolyte, it also needed a certain amount of mesopores. Mesopores and interconnections were important for the fast electrolyte transfer because they could provide more favorable paths for penetration and transportation of ions.[21]

The calculated structure parameters (total specific surface area, micro pore volume, total pore volume and major pore diameter) of pores are listed in Table 1. As shown in Table 1, the SSAs of DF-AC MG-AC and FC-AC calculated by BET method are about 911.2, 597.5 and 286.7 $m^2 g^{-1}$, respectively and corresponding total pore volume of DF-AC, MG-AC and FC-AC were 0.47, 0.25 and 0.11$cm^3 g^{-1}$ respectively. These results clearly explained that DF-AC exhibited higher surface area and pore volume. The high surface area and pore volume of DF-AC allowed facile accessibility of the electrode/electrolyte interface, resulting in efficient accumulation of charges or ions.

HK pore size distributions of as-prepared X-ACs were shown in Fig. 2b. It was clearly indicated that the pore distribution was mainly in the range of 1 ~ 3 nm. The hierarchical porous structure combining the abundant micropores and mesopores

might result in well match between adsorption and transportation of ions.

Table 1 Porosity parameters, element composition by XPS and capacitance of as-prepared X-ACs

Sample	C (at.%)	O (at.%)	S_{BET}[a] (m^2 g^{-1})	V_{mic}[b] (cm^3 g^{-1})	V_t[c] (cm^3 g^{-1})	D[d] (nm)	Capacitance (F g^{-1})
DF-AC	73.05	22.26	911.2	0.25	0.47	1.42	286.9
MG-AC	82.64	14.27	597.5	0.19	0.25	1.53	238.7
FC-AC	72.08	23.32	286.7	0.02	0.11	1.61	226.6

[a] BET surface area. [b] Micro pore volume. [c] Total pore volume. [d] HK pore size distributions

XRD and Raman spectroscopy were employed to investigate the crystalline structure of as-prepared X-ACs. The XRD patterns of as-prepared X-ACs were shown in Fig. 3a. As could be seen, all samples showed two weak diffraction peaks centered at 2θ = 24° and 43°, corresponding to (002) and (110) planes, respectively.

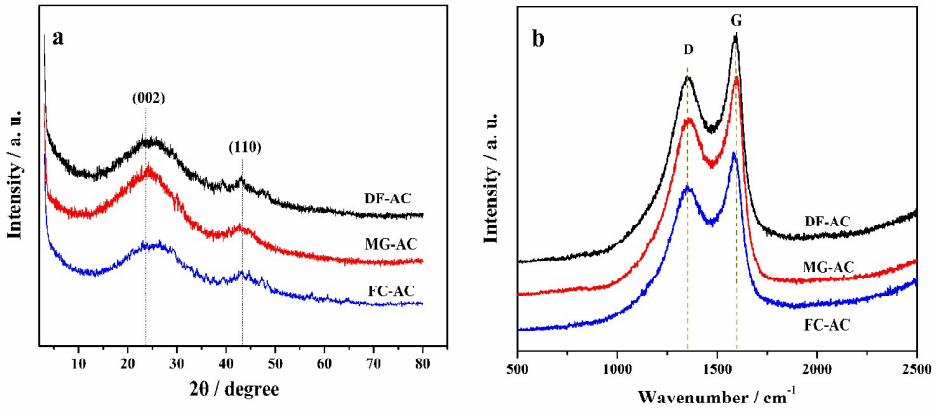

Fig. 3 XRD patterns (a) and Raman spectra (b) of as-prepared X-ACs

According to Scherrer's equation, the crystallite size (Lc) values of as-prepared X-ACs were calculated as 2.15 nm, 2.1 nm and 2.15 nm, respectively. Meanwhile, the inter planar distance (d_{002}) values of as-prepared X-ACs were about 0.389 nm, larger than that of graphite (0.335 nm), implying a random combination of graphitic and turbostratic stacking.[22] In addition, the peaks at 43° were relatively weak, suggesting that graphitic structure was only developed to a slight extent. Supporting evidence also came from Raman spectroscopic analysis as follows.

Raman spectra (Fig. 3b) clearly showed the well-known D-band peak at 1350 cm^{-1} (attributed to defected carbon crystallites) and G-band peak at 1590 cm^{-1} (attributed

to crystalline graphite). It was well known that the relative intensity of D-band and G-band (I_D/I_G) was proportional to the crystalline degree of carbon materials. I_D/I_G values of DF-AC, MG-AC and FC-AC were calculated as 1.17, 1.47 and 1.24, respectively, demonstrating that three kinds of as-prepared X-ACs had a low degree of graphitization and significant amount of disordered sections and defects. Compared with the I_D/I_G values of MG-AC and FC-AC, the value of DF-AC was lowest, indicating the highest graphitization degree of DF-AC. The results of Raman spectra analysis were consistent with XRD result above.

Shown in Fig. 4 were FTIR spectra of as-prepared X-ACs. The broad peak at 3430 cm^{-1} was attributed to O–H vibration of water absorbed on the surface of these materials.[23] The peak located at 1630 cm^{-1} was attributed to C=O vibration of carboxylic and carbonyls while the peak at 1410 cm^{-1} was assigned to C=C deformation vibration in phenols and O–H deformation vibration in carboxylic acids.[24,25] In addition, the stretching vibration of C–O bond caused the broad band at 1090 cm^{-1}.[26] FTIR analysis above clearly indicated the existence of oxygen species in as-prepared X-ACs.

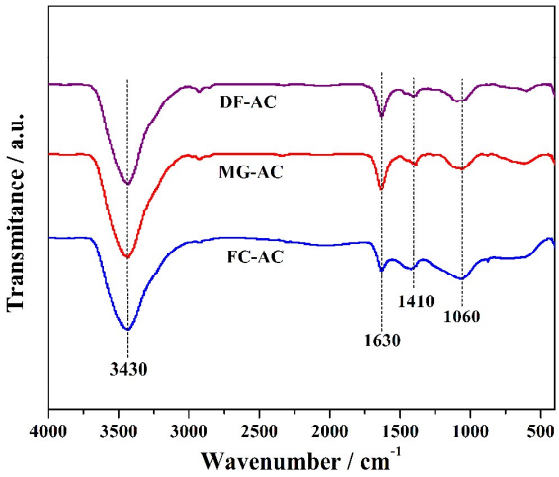

Fig. 4 FTIR spectra of as-prepared X-ACs

Surface chemical component and atomic percentage of the surface elements were evaluated by XPS analysis (Fig. 5). Obvious peaks of C1s (285 eV) and O1s (532 eV) were observed (Fig. 5a). Contents of element of C and O obtained from XPS analysis were listed in Table 1. C contents were found to be 73.05, 82.64, and 72.08

at.% for DF-AC, MG-AC and FC-AC, respectively, while O contents were 22.26, 14.27 and 23.32 at.%. Besides C and O, as-prepared X-ACs also contained around 3 ~ 5% other impurities (mainly Mg, Ca, K, etc, not listed here) which were not fully washed away by acid and water rinsing.

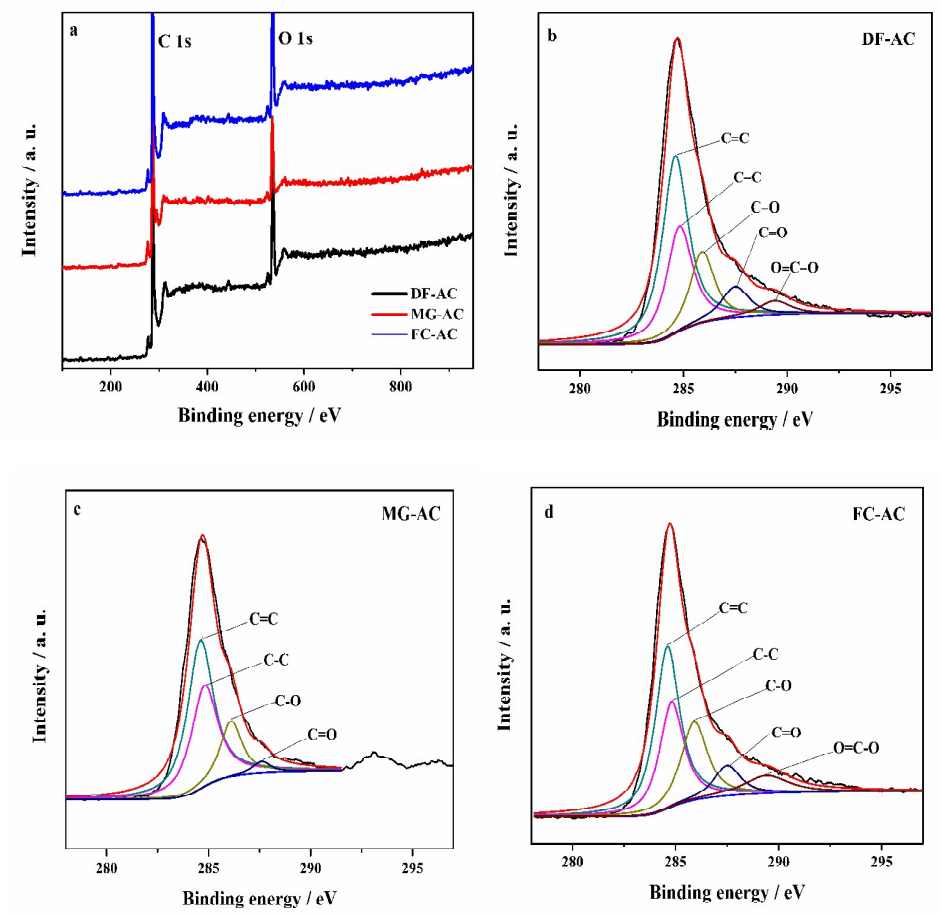

Fig. 5 XPS spectra of as-prepared X-ACs (a). C1s XPS spectra of as-prepared DF-AC (b), MG-AC (c) and FC-AC (d).

Shown in Fig. 5b, 5c and 5d were high-resolution C1s spectra of as-prepared X-ACs. Clearly, C1s spectra of DF-AC and FC-AC could be deconvoluted into five individual component peaks corresponding to C=C (284.6 eV), C–C (284.8 eV), C–O (285.9 eV), C=O (287.5 eV) and O=C–O (289.4 eV), while C1s spectrum of MG-AC could be deconvoluted into four individual component peaks corresponding to C=C (284.7 eV), C–C (284.8 eV), C–O (286.1 eV) and C=O (287.6 eV), fully indicating the existence of oxygen-containing groups in as-prepared X-ACs. These oxygen-containing

groups might be credited with electrochemical redox activity, which were considered to contribute to pseudo-capacitance.[27] In addition to pseudo-capacitance contribution, these surface oxygen-containing groups also played an important role in improving hydrophilicity and wettability of material surface and facilitating accessibility of electrolyte ions.[28]

3.2 Electrochemical performances of as-prepared X-ACs

Shown in Fig. 6 were CV curves of as-prepared X-AC electrodes in 2.0 mol l^{-1} KOH solution at scan rate of 20 mV s^{-1}. All curves exhibited quasi-rectangular shape, demonstrating behaviors of EDLCs with fast charge/discharge processes. According to the curves, DF-AC electrode presented better rectangular-like shape than MG-AC electrode and FC-AC electrode. This might be due to its high SSAs that benefited facile contact between electrode materials and electrolyte ions, enhancing capacitance.

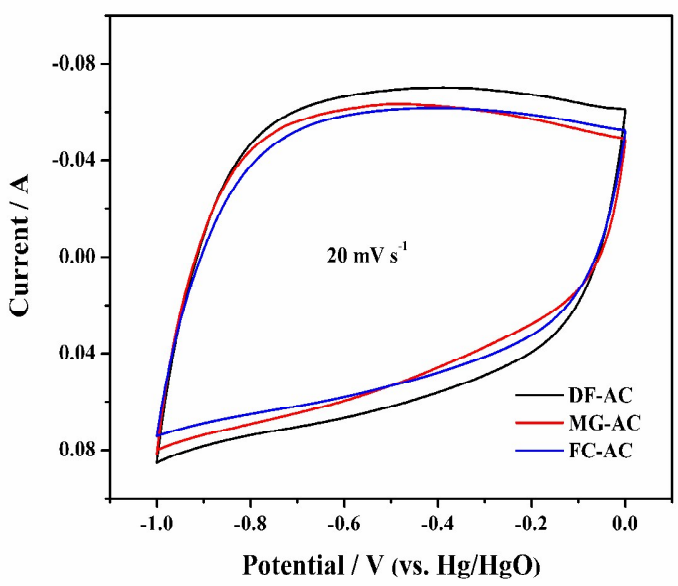

Fig. 6 CVs of as-prepared X-AC electrodes in 2.0 mol l^{-1} KOH solution over a potential range from –1.0 to 0 V at scan rate of 20 mV s^{-1}

Except for testing CV behaviors of as-prepared X-ACs at same scan rate, we also tested the detailed CV behaviors of DF-AC at different scan rates in 2.0 mol l^{-1} KOH solution. As shown in Fig. 7, when scan rate ranged from 5 to 30 mV s^{-1}, the quasi-rectangular shape could still remain, indicating excellent capacitive behaviors.[29]

When scan rate got to 50 mV s^{-1}, the curve became deformed. This phenomenon was attributed to the ohmic resistance for electrolyte motion in porous carbon, where storage charge had been recognized to be distributed for the double layer formation mechanism.

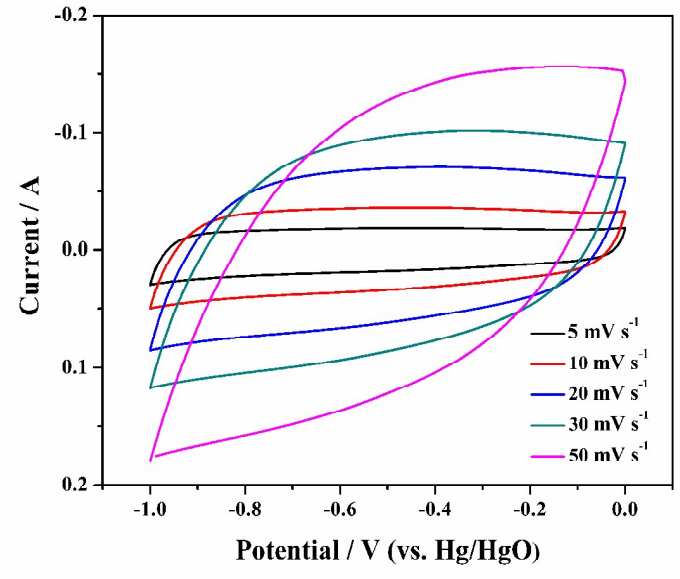

Fig. 7 CVs of DF-AC electrode in 2.0 mol l^{-1} KOH solution over a potential range from –1.0 to 0 V at different scan rates

Shown in Fig. 8 were GCD curves of as-prepared X-AC electrodes measured in 2.0 mol l^{-1} KOH solution at a current density of 0.5 A g^{-1} over a potential range from –1.0 to 0 V. It was obvious that GCD curves of all as-prepared X-ACs presented good linearity and symmetrical triangle, indicating good EDLCs behaviors. According to the formula of specific capacitance, $C = i \times \Delta t/(m \times \Delta V)$, where i was the discharge current (A), Δt the discharge time (s) and ΔV the potential window (V), the values of specific capacitance for DF-AC, MG-AC and FC-AC electrodes were calculated as 286.9 F g^{-1}, 238.7 F g^{-1} and 226.6 F g^{-1}, respectively, at current density of 0.5 A g^{-1}.

It was well known that mainly micropores played an essential role for charging an electrical double layer and had a great contribution to specific surface area. Thus micropores had an important effect on electric double-layer capacitance.

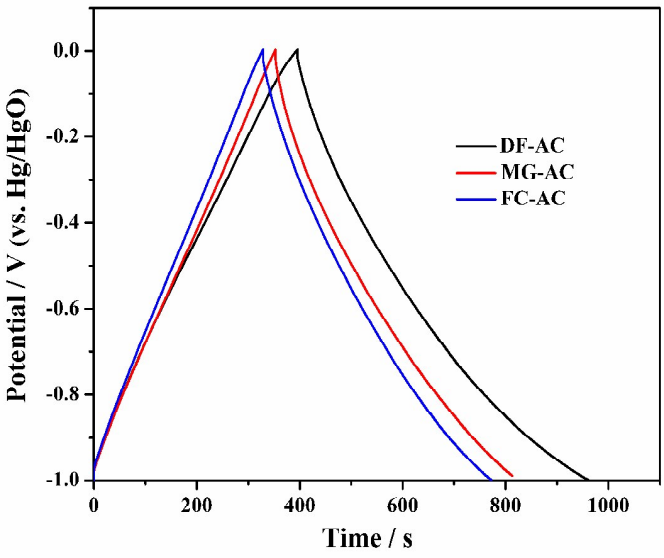

Fig. 8 GCD curves of as-prepared X-AC electrodes in 2.0 mol l^{-1} KOH solution over a potential range from –1.0 to 0 V at current density of 0.5 A g^{-1}

Besides, distribution and contribution of mesopores to the porous texture could enhance accessibility of electrolyte ions to the micropores. Mesopores could be also useful for sorption process if they had a small size below 5 nm. However, the excess in mesopore development, which was generally accompanied by decrease of total surface area, was detrimental to the charge storage.[30] Therefore, a suitable amount of mesopores played an important role to promote contact of ions and electrode. As a result, both micropores and mesopores had contribution on electric double-layer capacitance.

Moreover, capacitance also depended on the wettability of porous carbons by the electrolyte, which was determined by surface chemistry. The presence of oxygen functionalities on the carbon surface improved the wettability of material by an aqueous electrolyte resulting in a better penetration of ions within the porous structure. In addition, oxygen functionalities also induced pseudo-capacitance, leading to an enhancement of the capacitance.

As a result, capacitance depended on specific surface area and oxygen functionalities. Specific surface area depended on pore size and pore structure. Thus, pore size, pore structure and oxygen contents had co-contribution on capacitance.[31]

As listed in Table 1 above, it could clearly see that the specific surface area of FC-AC

was only 286.7 $m^2 g^{-1}$, which was less than that of MG-AC and DF-AC. The ratio of micro pore volume (0.02 $cm^3 g^{-1}$) and meso pore volume (0.09 $cm^3 g^{-1}$) was small, which had barely contribution to the specific surface area.[32] However, specific capacitance of FC-AC still reached 226.6 F g^{-1}, which was mostly attributed to the large content of oxygen atom (23.32 at.%) attached to the carbon network.

With the relatively high specific surface area (911.2 $m^2 g^{-1}$) and content of oxygen atom (22.26 at.%), the specific capacitance of DF-AC (286.9 F g^{-1}) was the highest among three samples.

Although the specific surface area of FC-AC (286.7 $m^2 g^{-1}$) was less than that of MG-AC (597.5 $m^2 g^{-1}$), the content of oxygen atom of FC-AC (23.32 at.%) was higher than that of MG-AC (14.27 at.%). Thus the values of specific capacitance of them were closely.

The above was the reason why the specific surface area of as-prepared X-ACs had great difference, whereas, the specific capacitance of them had small difference.

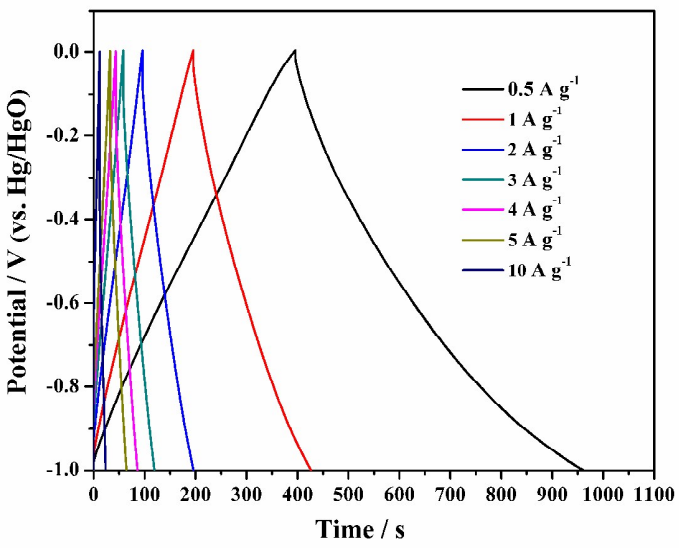

Fig. 9 GCD curves of DF-AC electrode in 2.0 mol l^{-1} KOH solution over a potential range from –1.0 to 0 V at different current densities

Shown in Fig. 9 were GCD curves of DF-AC electrode at different current densities. All curves were still highly symmetrical and linear at increased current densities from 0.5 A g^{-1} to 10 A g^{-1}, which was a typical characteristic of ideal capacitor. With increasing current density, specific capacitance decreased gradually from 286.9 F g^{-1}

at 0.5 A g^{-1} to 184 F g^{-1} at 10 A g^{-1}. The results indicated as-prepared DF-AC electrode had excellent capacitive behaviors.

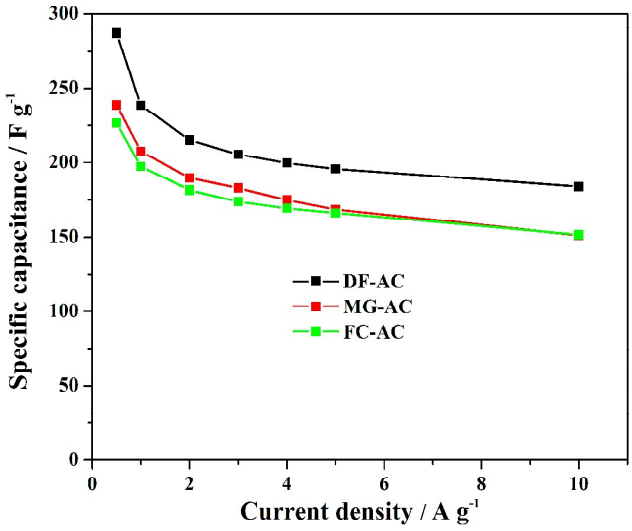

Fig. 10 Relationships between the specific capacitance value and current density of as-prepared X-AC electrodes

Depicted in Fig. 10 were values of specific capacitance calculated at different current densities from 0.5 to 10 A g^{-1}. It was found that specific capacitance decreased when current density enhanced, which was related to the increase of diffusion limitation.[33] At a high current density, electrolyte ions could not easily diffuse into pores, resulting in such a way that effective ion attachment occurred only at the surface of electrode.[34] However, when current density decreased, electrolyte ions could transport and diffuse into the pores easily. Therefore, compared with the capacitance at high current density, the capacitance at low current density was higher. According to Fig. 10, even at a current density of 10 A g^{-1}, DF-AC, MG-AC and FC-AC still maintained specific capacitances of 184 F g^{-1}, 151 F g^{-1} and 151 F g^{-1}, respectively.

This result above on the one hand might be due to the doping of oxygen, increasing hydrophilicity and polarity of carbon materials. Thus pseudo-capacitive behaviors had been induced. On the other hand, it might be due to the mesopores in as-prepared X-ACs, providing smooth and convenient ion transfer pathways for increasing contact areas between electrolyte and electrodes. Thus EDLCs behaviors

had been enhanced. The co-contribution of EDLCs and pseudo-capacitance made as-prepared X-ACs exhibit excellent electrochemical behaviors.

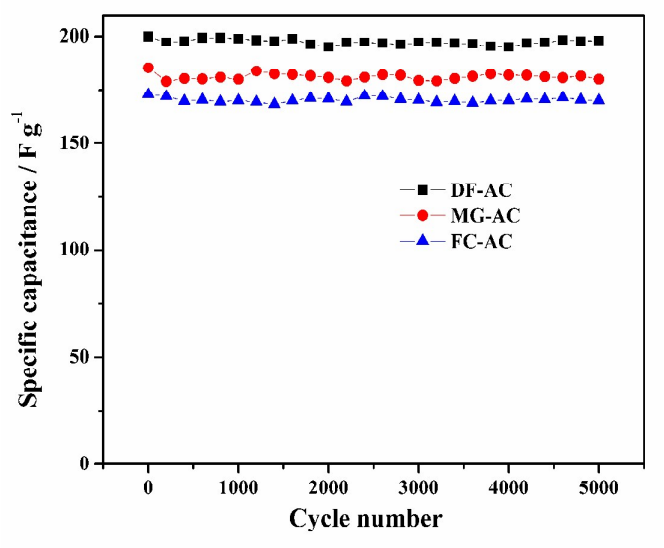

Fig. 11 Cycling stability of as-prepared X-AC electrodes at a charge/discharge current density of 4.0 A g^{-1} for 5000 cycles in 2.0 mol l^{-1} KOH solution

To evaluate cycle stability of as-prepared X-AC electrodes, continuous charge/discharge processes were conducted at a current density of 4.0 A g^{-1} for 5000 cycles in 2.0 mol l^{-1} KOH solution (Fig. 11). After 5000 continuous cycles, all as-prepared X-AC electrodes displayed excellent cycle stability with nearly 100% retention. The good electrochemical stability further confirmed the advantage of as-prepared X-ACs as electrode materials for supercapacitors.

4. Conclusions

In this paper, three kinds of oxygen-rich X-ACs were prepared via carbonization and KOH activation. High capacitances of as-prepared X-ACs were calculated as 286.9 F g^{-1}, 238.7 F g^{-1} and 226.6 F g^{-1} at 0.5 A g^{-1}, respectively, with nearly 100% retention capacitance over 5000 cycles at 4.0 A g^{-1}, which was attributable to large surface areas and O content of as-prepared X-ACs. Ours studies highlighted exciting possibility to utilize waste dragon fruit skin, momordica grosvenori skin and firmiana catkins to produce low cost electrode materials for high performance supercapacitors.

Acknowledgements

This work was supported by the Open Project of State Key Laboratory Cultivation Base for Nonmetal Composites and Functional Materials (11zxfk26) and the Postgraduate Innovation Fund Project from Southwest University of Science and Technology (15ycx010). Also we were grateful for the help of Analytical and Testing Center of Southwest University of Science and Technology.

References

1 W. Lei, P. He, S. S. Zhang, F. Q. Dong and Y. J. Ma, *J. Power Sources*, 2014, 266, 347-352.

2 W. Lei, P. He, Y. H. Wang, X. Q. Zhang, A. Xia and F. Q. Dong, *Compos. Sci. Technol.*, 2014, 102, 82-86.

3 Y. H. Wang, P. He, X. M. Zhao, W. Lei and F. Q. Dong, *J. Solid State Electrochem.*, 2014, 18, 665-672.

4 K. M. Ashish and R. Sundara, *J. Phys. Chem. C*, 2011, 115, 14006-14013.

5 M. Zeiger, N. Jackel, M. Aslan, D. Weingarth and V. Presser, *Carbon*, 2014, 84, 584-598.

6 D. Pech, M. Brunet, H. Durou, P. Huang, V. Mochalin and Y. Gogotsi, *Nat. Nanotechnol.*, 2010, 5, 651-654.

7 H. Wang, H. B. Feng and J. H. Li, *Small*, 2014, 10, 2165-2181.

8 Z. G. Wang, Z. G. Wu, G. D. Benedetto, J. L. Zunino and S. Mitra, *Carbon*, 2015, 91, 103-113.

9 D. B. Wang, Z. Geng, B. Li and C. M. Zhang, *Electrochim. Acta*, 2015, 173, 377-384.

10 Y. H. Wang, C. C. Wang, W. Y. Cheng and S. H. Lu, *Carbon*, 2013, 69, 287-293.

11 H. B. Feng, Y. M. Li and J. H. Li, *RSC Adv.*, 2012, 2, 6988-6993.

12 C. Peng, X. B. Yan, R. T. Wang, J. W. Lang, Y. J. Ou and Q. J. Xue, *Electrochim. Acta*, 2013, 87, 401-408.

13 X. He, P. Ling, J. Qiu, M. Yu, X. Zhang, C. Yu and M. Zheng, *J. Power Sources*, 2013, 240, 109-113.

14 J. Jiang, L. Zhang, X. Wang, N. Holm, K. Rajagopalan, F. Chen and S. G. Ma, *Electrochim. Acta*, 2013, 113, 481-489.

[15] H. Chen, H. Wang, L. Yang, Y. Xiao, M. Zheng, Y. Liu and H. Fu, *Int. J. Electrochem. Sci.*, 2012, 7, 4889-4897.

16 H. Jin, X. M. Wang and A. R. Gu, *Mater. Focus*, 2013, 2, 105-112.

17 T. E. Rufford, D. Hulicova-Jurcakova, K. Khosla, Z. H. Zhu and G. Q. Lu, *J. Power Sources*, 2010, 195, 912-918.

18 S Kanlayanarat, A. L. Acedo and C. WongsAree, *Acta Hortic.*, 2013, 989, 271-278.

19 R. Di, M. T. Huang and C. T. Ho, *J. Agric. Food Chem.*, 2011, 59, 7474-7481.

20 Q. Wang, Q. Cao, X. Wang, B. Jing, H. Kuang and L. Zhou, *J. Power Sources*, 2013, 225, 101-107.

21 P. A. Johns, M. R. Roberts, Y. Wakizaka, J. H. Sanders and J. R. Owen, *Electrochem. Commun.*, 2009, 11, 2089-2092.

22 M. Sevilla and A. B. Fuertes, *Carbon*, 2013, 56, 155-166.

23 Y. Guo and D. A. Rockstraw, *Microporous Mesoporous Mater.*, 2007, 100, 12-19.

24 C. J. Chen, P. C. Zhao, Y. M. Huang, Z. F. Tong and Z. X. Li, *J. Inorg. Organomet. Polym. Mater.*, 2013, 231, 1201-1209.

25 G. Mastrolonardo, O. Francioso, M. D. Foggia, S. Bonora, C. Forte and G. Certini, *J. Soils Sediments*, 2015, 15, 769-780.

26 M. Anbia and S. E. Moradi, *Korean J. Chem. Eng.*, 2012, 29, 743-749.

27 Q. H. Liang, L. Ye, Z. H. Huang, Q. Xu, Y. Bai, F. Y. Kang and C. Yuan, *Nanoscale*, 2014, 6, 13831-13837.

28 K. Lee, D. Kim, Y. Yoon, J. Yang, H. G. Yun, I. K. You and H. Lee, *RSC Adv.*, 2015, 5, 60914-60919.

29 J. T. Zhang, L. Y. Gong, K. Sun, J. C. Jiang and X. G. Zhang, *J. Solid State Electrochem.*, 2012, 16, 2179-2186.

30 G. Gryglewic, J. Machnikowski, E. L. Grabowska, G. Lotab and E. Frackowiak, *Electrochim. Acta*, 2005, 50, 1197-1206.

31 Y. D. Chen, B. Huang, M. J. Huang and B. Q. Cai, *J. Taiwan Inst. Chem. Eng.*, 2011, 42, 837-842.

32 S. M. Jung, D. L. Mafra, C. T. Lin, H. Y. Jung and J. Kong, *Nanoscale*, 2015, 7, 4386-4393.

33 L. Sun, C. G. Tian, M. T. Li, X. Y. Meng, L. Wang, R. H. Wang, J. Yin and H. G. Fu, *J. Mater. Chem. A*, 2013, 1, 6462-6470.

34 M. D. Chen, X. Y. Kang, T. Wumaier, J. Q. Dou, B. Gao, Y. Han, G. Q. Xu, Z.

Liu and L. Zhang, *J. Solid State Electrochem.*, 2013, 17, 1005-1012.

Graphical abstract

Oxygen-doped activated carbons derived from three kinds of biomasses: Preparation, characterization and performance as electrode materials for supercapacitors

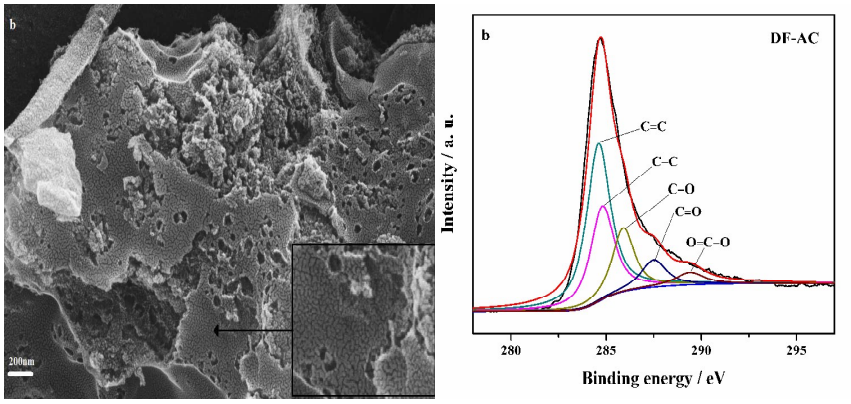

Shown in left was SEM image of MG-AC. Observed were irregular, amorphous structure and a mountain of channels. Shown in right were C1s XPS spectra of as-prepared DF-AC. Clearly, C1s spectra of DF-AC could be deconvoluted into five individual component peaks corresponding to C=C (284.6 eV), C–C (284.8 eV), C–O (285.9 eV), C=O (287.5 eV) and O=C–O (289.4 eV), fully indicating the existence of oxygen-containing groups in as-prepared activated carbon.